Ⅲ-3

Chemistry

BL1U

Induced Chirality by Circularly Polarized UV Light for Photofunctional Organic/Inorganic Hybrid Materials

T. Akitsu[1], N. Sunaga[1], N. Ishida[1], M. Ito[1], T. Konomi[2] and M. Kato[2]
[1]*Department of Chemistry, Faculty of Science, Tokyo University of Science, Tokyo 162-8601, Japan*
[2]*UVSOR Facility, Institute for Molecular Science, Okazaki 444-8585, Japan*

Photofunctional organic/inorganic hybrid materials containing chiral Schiff base Ni(II), Cu(II), and Zn(II) complexes involving azobenzene moiety have been prepared and investigated (supra)molecular orientation induced by linearly polarized UV light irradiation (optical dichroism, namely Weigert effect) with polarized electronic and IR spectroscopy or induced by circularly polarized UV light irradiation (supramolecular chirality) with CD spectra [1-3]. However, in oriented samples, artifact CD peaks prevents from obtaining proper data generally. So we have employed wavelength selective UV light generated by UVSOR BL-1U beamline. At the first term, circularly polarized UV light induced chiral supramolecular orientation was observed with difference CD spectra (before and after UV irradiation), while at the second term, that linearly polarized UV light induced changes resulted in little changes of CD spectra was confirmed as control experiments.

New diastereomers of (achiral or chiral) Schiff base Ni(II), Cu(II), and Zn(II) complexes with or without azobenzene moiety in ligands were prepared as PMMA cast films (namely total 6 types of organic/inorganic photofunctional hybrid materials). These samples were irradiated linearly or circularly polarized UV light at UVSOR BL-1U and compared CD spectra before and after UV light irradiation to confirm molecular orientation inside of the hybrid materials.

Circularly polarized UV light at 260, 318, and 380 nm was irradiated for (0), 3, 5, and 8 min and differences of CD spectra (considered blank data to remove the effect artifact peaks) indicated increasing CD peaks which suggested that chiral supramolecular orientation was induced. Light at 260 nm was effective for inducing bands at about 300 nm for all complexes (in addition about 400 nm only for Zn(II) complex). Light at 318 and 380 nm was effective for inducing bands at about 300 and 500 nm for all complexes (in addition about 500 nm for Ni(II) and Zn(II) complexes, and about 700 nm for Cu(II) complex).

On the other hand, similar discussion by difference CD spectra before and after linearly polarized UV light irradiation at selective wavelengths suggested that no CD peaks could be observed at long-wavelength region without noise peaks.

Generally in isotropic environment like solutions, proper CD spectra can be obtained for chiral metal complexes, which was ascribed to molecular chirality. While no CD spectra could be observed for achiral metal complexes. However, it was well known that in anisotropic environment like oriented samples (for example, solid state or well-oriented films) not only proper CD bands but also artifact CD bands could be observed. In difference CD spectra, artifact peaks were cancelled when changes about chirality did not occurred even if there are molecular or supramolecular chirality. In other words, although linearly polarized UV light induced optical anisotropy of metal complexes in hybrid materials, supramolecular chiral ordering was not influenced even for chiral metal complexes.

In conclusion, emerging CD peaks in difference CD spectra is attributed to supramolecular helical orientation induced by circularly polarized UV light irradiation for achiral as well as chiral metal complexes. Additionally, UV light of certain wavelengths can effectively induced molecular orientation.

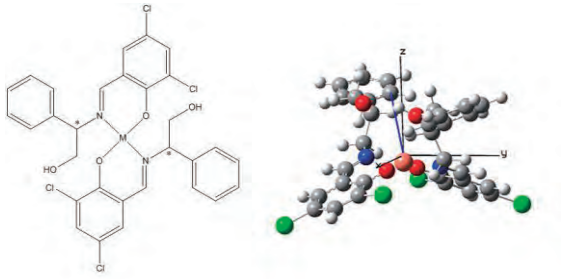

Fig. 1. Chiral Schiff base metal complex without azobenzene moiety [left] and its optimized structure [left].

[1] M. Ito and T. Akitsu, Contemporary Engineering Sciences **7** (2014) 869.
[2] N. Hariu, M. Ito and T. Akitsu, Contemporary Engineering Sciences **8** (2015) 57.
[3] N. Sunaga, S. Furuya, M. Ito, C. Kominato and T. Akitsu, *Computational Chemistry: Theories, Methods and Applications* (Nova Science Publishers, Inc., NY, USA, 2014) 85.

BL1U

Photoionization Study of Helium Atoms Using Variable Polarization Undulator

T. Kaneyasu[1], Y. Hikosaka[2], T. Konomi[3], M. Katoh[3], H. Iwayama[3] and E. Shigemasa[3]

[1]*SAGA Light Source, Tosu 841-0005, Japan*

[2]*Department of Environmental Science, Niigata University, Niigata 950-2181, Japan*

[3]*UVSOR Facility, Institute for Molecular Science, Okazaki 444-8585, Japan*

The n_{th} harmonic radiation from a helical undulator carries orbital angular momentum (OAM) of $(n\text{-}1)\hbar$ per photon [1,2]. This accelerator-based method efficiently generates the OAM photon beam in a wide wavelength range. The APPLE-II undulator U1 in UVSOR storage ring is suitable for generating the OAM photon beam in the EUV region. We are planning to investigate the interaction of the OAM photon with gas-phase atoms in which violation of the dipole selection rules is predicted [3].

For the feasibility study on performing the gas-phase experiment by using the undulator U1, we constructed a test endstation equipped with the photoelectron imaging spectrometer [4] as shown in Fig.1. As a performance test of the experimental setup, we measured the angular distributions of the He 1s photoelectrons using the fundamental radiation with horizontal linear and circular polarization. The peak energy of the undulator radiation was roughly set to 30 eV. The experiments were performed during the machine study using the single-bunch mode. For eliminating the background signals due to secondary electrons emitted from the repeller plate of the imaging spectrometer, we applied the time gate signal to the detector system.

Figure 2 shows the photoelectron images which correspond to the projections of the three-dimensional velocity distributions. The photon propagation direction is along the Y-axis, while the electric vector of the horizontally polarized radiation is parallel to the X-axis. The images present broad structures corresponding to the photoelectrons having 5 eV kinetic energy. The broadness of the photoelectron structures is mainly due to the bandwidth (~2 eV fwhm) of the undulator radiation.

Figure 3 shows the photoelectron angular distributions converted from the images in Fig. 2. using the peeling-analysis. The measured angular distributions are in reasonable agreement with those calculated for the dipole asymmetry parameter β=2. This result confirms the usefulness of the present method for measuring the photoelectron angular distributions. We note that small deviations from the β=2 patterns are probably due to image distortions resulting from the stray magnetic field and imperfection in the background subtraction. For the experiment on the OAM photoionization, we are preparing a magnetic shield and a modified repeller plate for the imaging spectrometer, both of which are essential for improving the image quality.

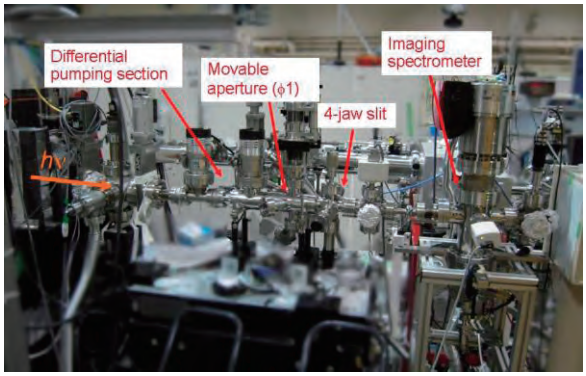

Fig. 1. Photo of the experimental setup constructed at BL1U.

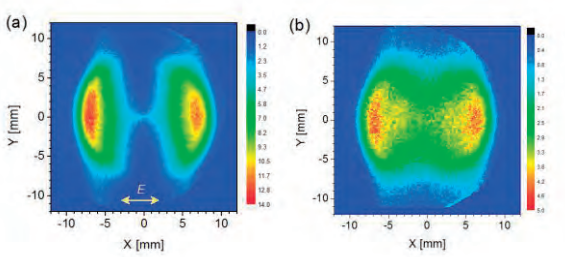

Fig. 2. He 1s photoelectron images measured for (a) horizontal linear and (b) circular polarization.

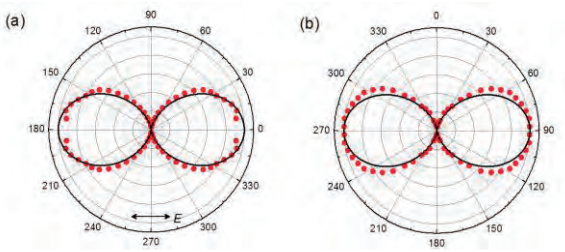

Fig. 3. He 1s photoelectron angular distributions measured for (a) horizontal linear and (b) circular polarization. Circles: experimental data, Solid curves: calculation for β=2.

[1] S. Sasaki and I. McNulty, Phys. Rev. Lett. **100** (2008) 124801.

[2] J. Bahrdt *et al.*, Phys. Rev. Lett. **111** (2013) 034801.

[3] A. Picón *et al.*, New J. Phys. **12** (2010) 083053.

[4] Y. Hikosaka and E. Shigemasa, J. Electron Spectrosc. Relat. Phenom. **148** (2005) 5.

BL3U

In Situ Soft X-Ray Absorption Spectroscopy Applied to Solid-Liquid Heterogeneous Cyanopyrazine Hydration on Titanium Oxide Catalyst

H. Yuzawa, M. Nagasaka and N. Kosugi
Institute for Molecular Science, Okazaki 444-8585, Japan

In situ observation of liquid substrate conversion process in solid-liquid heterogeneous catalytic reaction is difficult because the bulk liquids (substrate and/or solvent) hinder the objective spectral change [1]. This type of spectroscopy has been often carried out by using ATR-IR and NMR, but these methods still have some problems of the sensitivity and the overlap of the target spectral signals.

We have developed a transmission-type in situ liquid flow cell, which is able to optimize easily the liquid layer thickness for the soft X-ray XAS [2] and demonstrated that this spectroscopic method is effective to clarify the local structure of various liquid solutions [3]. Thus, in the present study, we have applied this method to time and temperature dependent in situ XAS measurements of solid-liquid heterogeneous cyanopyrazine hydration to produce pyrazinamide (PzCN + H_2O → $PzCONH_2$) on TiO_2 catalyst [4].

The experiments were carried out in BL3U. Suspension of catalyst was prepared by mixing of PzCN (3 ml, 0.78 M), EtOH (5 ml), H_2O (35 ml) and TiO_2 (0.15 g). The suspension of thin layer (< 1 μm thickness) was sandwiched between two 100 nm-thick Si_3N_4 membranes for C K-edge XAS (SiC membranes for N K-edge XAS). Then, the measurement was carried out under various reaction temperatures from 323.2 to 344.5 K.

Figure 1a shows the C K-edge XAS spectra of PzCN and $PzCONH_2$ at 298K, and the hydration of cyanopyrazine at 335 K. Three absorption peaks (285.4, 286.0 and 286.6 eV) are observed in PzCN (red line) and one absorption peak (285.3 eV) in $PzCONH_2$ (blue line) are observed. All these peaks are assigned to the C1s → π* excitation. In the spectra of PzCN hydration (green lines), the intensity ratio of the absorption peaks varies with the reaction time, corresponding to the production of $PzCONH_2$. Figure 1b shows a logarithmic plot for the normalized XAS intensity of PzCN, which is obtained from the fitting analysis of Fig. 1a (green lines) by using the standard spectra of PzCN and $PzCONH_2$. This plot shows linear relationship to the reaction time, indicating that the observed catalytic reaction is the first-order reaction for the concentration of PzCN and the slope of the line is a reaction rate constant. The same results are obtained from C K-edge XAS at other temperatures and N K-edge XAS. Furthermore, the obtained rate constants show linear relationship in the Arrhenius plot (E_a = 80 kJ/mol). Thus, it is confirmed that this analytical procedure is reasonable.

We have compared this method with FT-IR spectroscopy, which is typically used for the in situ observation of catalytic reaction. FT-IR cannot detect the characteristic peaks of PzCN (Fig. 2, purple line) in the PzCN solution used for the catalytic reaction (red line) because of the hindrance by the absorption of H_2O and EtOH. Therefore, in situ soft X-ray XAS has a merit to detect minor liquid components in the catalytic reaction.

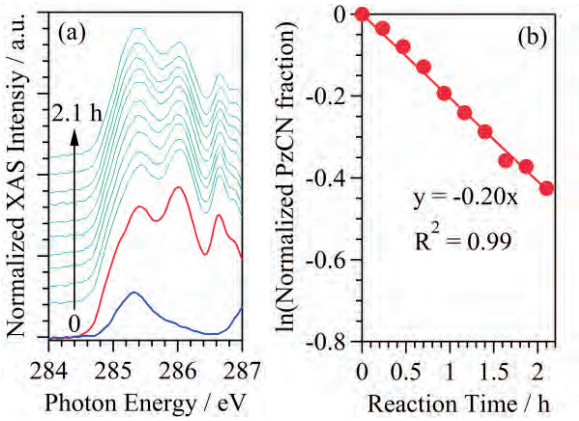

Fig. 1. (a) C K-edge XAS spectra for the PzCN (0.78 M) (red line) and $PzCONH_2$ (0.20 M) suspensions (blue line) at 298 K and catalytic hydration of PzCN on TiO_2 (green lines) at 335 K. (b) A logarithmic plot of the normalized XAS intensity of PzCN obtained from the fitting analysis of green lines in (a).

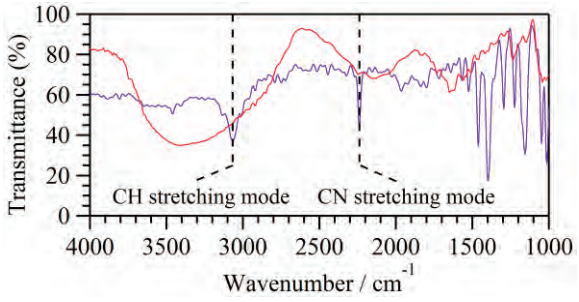

Fig. 2. FT-IR spectra in transmission mode of pure PzCN (purple line) and 0.78 M PzCN solution (red line) used in the catalytic hydration. They were measured by using the same liquid cell as in the XAS.

[1] F. Zaera, Chem. Rev. **112** (2012) 2920.
[2] M. Nagasaka *et al.*, J. Electron Spectrosc. Relat. Phenom. **177** (2010) 130.
[3] M. Nagasaka *et al.*, J. Phys. Chem. B **118** (2014) 4388.
[4] H. Yuzawa *et al.*, J. Phys. Chem. C, accepted.

BL3U

Electronic Structure of Interfacial Water on Nanodiamonds in Colloidal Dispersions

T. Petit[1], H. Yuzawa[2], M. Nagasaka[2], R. Yamanoi[3], E. Osawa[3], N. Kosugi[2] and E. F. Aziz[1,2,4]

[1] *Institute of Methods for Materials Development, Helmholtz-Zentrum Berlin, Albert-Einstein-Str. 15, 12489 Berlin, Germany*

[2] *Institute for Molecular Science, Myodaiji, Okazaki 444-8585, Japan*

[3] *NanoCarbon Research Institute, AREC, Shinshu University, Ueda 386-8567, Japan*

[4] *Freie Universität Berlin, FB Physik, Arnimallee 14, 14195 Berlin, Germany*

The organization of water molecules close to solid surfaces or around proteins differs significantly from pure water [1]. Reorganization of solvent molecules is likely to occur around colloidal nanoparticles and its understanding is of outermost importance to better estimate their reactivity and interaction with biological moieties in aqueous environment. Nevertheless, the structure of solvent molecules around nanomaterials in colloidal dispersion remains largely unexplored. Nanodiamonds (NDs) are of particular interest for the investigation of interfacial water since the existence of an ordered water shell ranging from 2 to 4 water layers was recently suggested.

The experiments were performed at BL3U in UVSOR-III. Aqueous dispersions of NDs with different sizes (ranging from 3 to 18 nm) and surface chemistries were characterized by X-ray absorption spectroscopy (XAS) in pure transmission using a flow cell described elsewhere [2]. By comparing these XA spectra at oxygen K edge to pure water spectra, the organization of water molecules in hydration layers of NDs could be investigated.

Orientation of water molecules in the first solvation shell is found to depend on the Zeta potential of NDs as seen by changes in the pre-edge feature of O K edge XA spectra. In particular, more hydrogen bonds are broken at the surface of negatively-charged NDs due to electrostatic interaction with carboxylate groups while water molecules donating two hydrogen bonds are dominant on positively-charged NDs.

Furthermore a long range order, having an electronic signature close to high density amorphous ice, was evidenced. As seen on Fig. 1, the X-ray absorption increases dramatically at high NDs concentration. This increase is significant compared to aqueous ionic solution. The electronic structure of water is extremely different from bulk water due to the strong contribution from interfacial water layers around NDs. Unlike ions, NDs are too large to be engulfed in a hydration cage which would break a limited amount of hydrogen bonds [3]. At the same time, they are small enough to offer a large interface and the surface polarization orients water molecules around them. It has to be noted that dispersions of detonation NDs at concentration around 8-10 wt% forms highly viscous gel, which may be a consequence of the long range ordering of water molecules around NDs.

We could evidence that the electronic structure of interfacial water layers on NDs is very uncommon. The long range ordering of water molecules on their surface may explain the high affinity of NDs for proteins adsorption or participate to their low toxicity. These results have recently been submitted for publication.

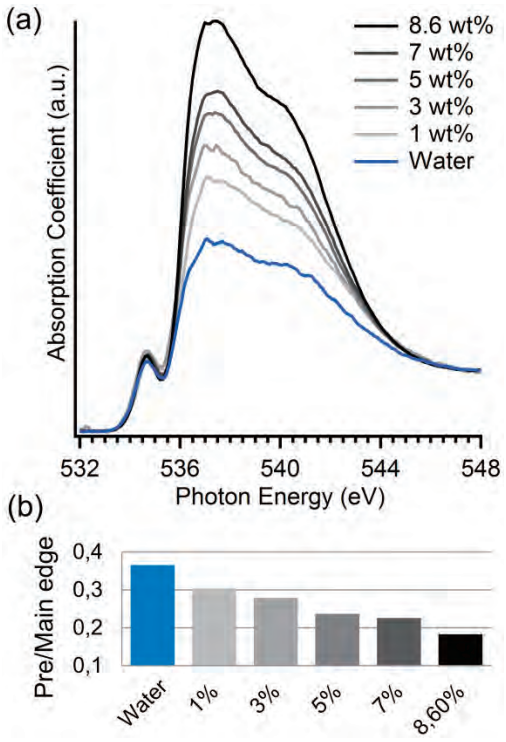

Fig. 1. (a) XAS of oxygen K-edge from water and aqueous dispersion of NDs at different concentrations ranging from 1 to 8.6 wt%. (b) Pre/Main-edge ratios for the different concentrations.

[1] J.-J. Velasco-Velez *et al*., Science **346** (2014) 831.
[2] M. Nagasaka *et al*., J. Phys. Chem. C **117** (2013) 16343.
[3] D. Chandler, Nature **437** (2005) 640.

BL3U

Fluorination-Dependent Molecular Orbital Occupancy in Perfluorocarbons

T. Brandenburg[1,2], T. Petit[1], A. Neubauer[1], K. Atak[1,2], M. Nagasaka[3], R. Golnak[1,2], N. Kosugi[3] and E. F. Aziz[1,2,3]

[1] *Institute of Methods for Material Development, Helmholtz-Zentrum Berlin für Materialien und Energie, Albert-Einstein-Straße 15, 12489 Berlin, Germany*

[2] *Department of Physics, Freie Universität Berlin, Arnimallee 14, 14195 Berlin, Germany*

[3] *Institute for Molecular Science, Okazaki 444-8585, Japan*

The family of perfluorocarbons has a wide range of applications in biomedicine and physical chemistry due to their extraordinary properties. Many liquid perfluorocarbons are known to show high density, high viscosity as well as an especially high gas solubility, and are often chemically and biological inert. Their ability to dissolve gases and their biological inertness are exploited in the main applications, such as tissue oxygenation or post-operative treatment.

The perfluoro effect, inherent to all perfluorocarbons, describes the energetic shifts of the spectral features upon complete fluorination of hydrocarbons. This also led to a general rule for the dimensions of the energetic shifts depending on σ- or π-character of the molecular orbitals (MO). Hence, this effect can be used for experimental orbital classification. In this context, a few experimental studies have already been performed in the 1970s. Many of them were based on photoelectron spectroscopy. Since then, more complex theoretical models and the introduction of new experimental techniques give opportunities to investigate perfluorocarbons.

Through the measurements performed at the beamline BL3U in UVSOR-III we could obtain X-ray absorption (XA) spectra of several perfluorocarbons with sufficient signal intensity and without experimental saturation effects. These spectra are complemented by resonant inelastic X-ray scattering (RIXS) spectra obtained at the LiXedrom endstation in BESSY II (Germany) [1, 2].

We could present fundamental insight into the energetic shift induced by fluorination, the so-called perfluoro effect, and a comprehensive picture of the electronic structure of decalin as the parent hydrocarbon molecule for perfluorodecalin based on the XA, X-ray emission (XE) and RIXS spectroscopic data [3]. In addition DFT calculations for decalin, perfluorodecalin and stepwise fluorinated decalin derivatives were performed. We observed a change in occupancy of MOs occurring for the fluorinated hydrocarbons when reaching complete fluorination in PFD.

This MO alteration may be one of the main reasons for the chemical and biological inertness of the ring-shaped perfluorodecalin compared to decalin and the corresponding partially fluorinated hydrocarbons. Interestingly, the discovered orbital change in the XA spectra could also be observed in the XE spectra in a complementary way. To the best of our knowledge, the observability of the perfluoro effect via XE spectra was confirmed for the first time, and the orbital change originating from unoccupied decalin to occupied PFD MOs was also discussed in relation to the well-known high electronegativity of fluorine atoms. Hence, the validity of this concept and its extension to linear and also larger perfluoro systems is of particular interest for a better understanding of the special properties of perfluoro compounds and their application development.

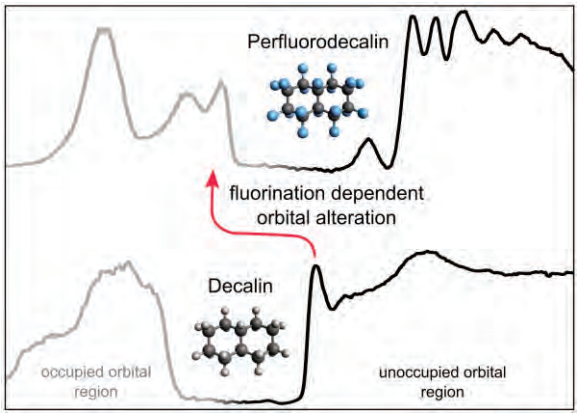

Fig. 1. Sketch of the acquired data with an indication of the discovered orbital alteration.

[1] K. M. Lange *et al.*, Phys. Rev. B **85** (2012) 155104.
[2] C. Jung *et al.*, Nucl. Instrum. Methods Phys. Res. Sect. Accel. Spectrometers Detect. Assoc. Equip. **467-468** (2001) 485.
[3] T. Brandenburg *et al.*, under review.

BL3U

Local Structures of Liquid Benzene Studied by Temperature-Dependent C K-Edge Soft X-Ray Absorption Spectroscopy

M. Nagasaka[1], H. Yuzawa[1], K. Mochizuki[1,2], E. Rühl[3] and N. Kosugi[1]
[1] *Institute for Molecular Science, Myodaiji, Okazaki 444-8585, Japan*
[2] *Department of Chemistry, Okayama University, Okayama 700-8530, Japan*
[3] *Physikalische Chemie, Freie Universität Berlin, Takustr. 3, D-14195 Berlin, Germany*

Benzene is liquid at room temperature. We reported C K-edge X-ray absorption spectroscopy (XAS) of benzene clusters formed by supersonic gas expansion method, and investigated molecular interaction from the energy shift of C 1s → π* peak of benzene clusters from benzene gas [1]. We also investigated the energy shift of C K-edge XAS of solid benzene, which was grown in multilayers on Ru(0001) crystal surface under vacuum condition revealing the gas-to-solid shift in the C 1s-regime [2]. However, the molecular interaction in liquid benzene has not yet been investigated. In the present study, we have measured C K-edge XAS of liquid benzene at different temperatures, and studied the temperature effect of the molecular interaction.

The experiments were performed at BL3U in UVSOR-III. XAS spectra of liquid samples were measured by a transmitted-type liquid flow cell [3]. The liquid layer was sandwiched between two 100 nm-thick Si_3N_4 membranes. The thickness of the liquid layer is controllable between 20 nm and 2000 nm by adjusting the He pressure.

Figure 1 shows C K-edge XAS of gaseous and liquid benzene at different temperatures. The C 1s → π* peak shows adiabatic (0, 0) transition and vibrational fine structures at higher photon energy. Figure 2 shows the energy shifts of (0, 0) transition peaks of liquid benzene from gaseous benzene as a function of temperature. The π* peak shows a shift to lower photon energy by increasing the temperature of the sample. The energy shift of liquid benzene relative to the gas phase is 29.4 meV at 25.3 ºC. This shift is smaller than in solid benzene and clusters, which is 55 meV [2] and 70 meV [1], respectively.

The energy shift of the π* peak is caused by the balance between the red-shift effect by induced polarization with surrounding molecules and the blue-shift effect by exchange interaction between the unoccupied π* orbital with surrounding molecules [4]. Exchange interaction is effective in the short range, so that the peak is shifted in condensed benzene to lower photon energy when the molecular distance becomes longer. This is consistent with the fact that benzene molecules are increasingly separated from each other in the liquid as the temperature is raised. Furthermore, the radial distribution function between benzene molecules changes as a function of temperature as evidenced by molecular dynamics simulations. We have also investigated the interactions between benzene molecules by exciting the C-H out-of-plane and C-H stretching vibration mode by infrared spectroscopy. In the future, we will discuss the molecular interaction in liquid benzene by correlating C K-edge XAS results with infrared spectroscopy and molecular dynamics simulations.

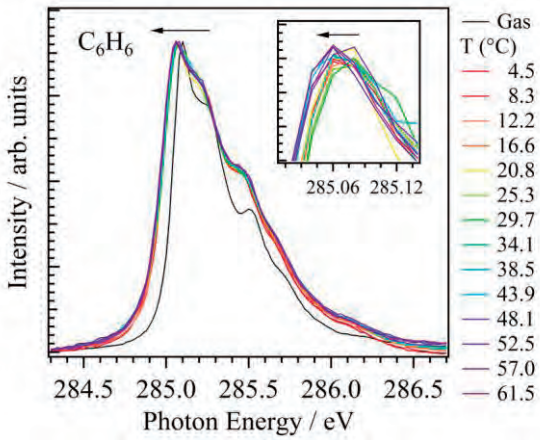

Fig. 1. C K-edge XAS of gaseous and liquid benzene at different temperatures. The inset shows the maximum of the C 1s → π* transition in greater detail.

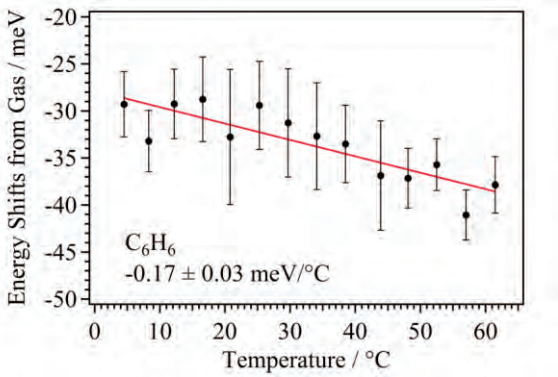

Fig. 2. Energy shifts of C 1s → π* (0, 0) transition peak of liquid benzene relative to gaseous benzene as a function of temperature.

[1] I. L. Bradeanu *et al.*, Phys. Chem. Chem. Phys. **8** (2006) 1906.
[2] R. Flesch *et al.*, Phys. Chem. Chem. Phys. **14** (2012) 9397.
[3] M. Nagasaka *et al.*, J. Electron Spectrosc. Relat. Phenom. **177** (2010) 130.
[4] M. Nagasaka *et al.*, J. Electron Spectrosc. Relat. Phenom. **183** (2011) 29.

BL3U

Optimization of the Sample Position of the Liquid Thin Layer for Soft X-Ray Absorption Spectroscopy

M. Nagasaka, H. Yuzawa, T. Horigome and N. Kosugi
Institute for Molecular Science, Okazaki 444-8585, Japan

In order to measure X-ray absorption spectroscopy (XAS) of liquid samples in transmission mode, it is necessary to control the liquid thickness. Recently, we have developed a transmitted-type liquid flow cell to measure XAS of liquid samples [1]. The liquid layer is sandwiched between two Si_3N_4 membranes, and the thickness is controllable from 20 nm to 2000 nm by adjusting helium pressures outside the membranes. However, in this system, it is not able to control the sample position and it is difficult to confirm the flatness, or uniform thickness, of the thin liquid layer. In the present study, we have developed an XAS measurement system to sweep the position of the liquid layer, and have measured O K-edge XAS of liquid water at different positions to find a flat area of the sample.

The experiments were performed at BL3U in UVSOR-III. The system consists of ultrahigh vacuum and atmospheric helium conditions, which are separated by Si_3N_4 membranes (0.2 × 0.2 mm^2). The liquid cell that is sandwiched between two Si_3N_4 membranes (2 × 2 mm^2) is in atmospheric condition, and is swept to different positions. XAS in transmission mode is measured by a photodiode detector set behind the liquid cell. This system also equips a silicon drift detector to measure XAS in fluorescence mode.

Figure 1 shows O K-edge XAS of liquid water at different sample positions. The inset of Fig. 2 shows the images of X-ray transmission at 550 eV. O K-edge XAS were measured by scanning the sample positions shown in the arrow. O K-edge XAS shows three features: The pre-edge at 535 eV, main-edge at 537 eV, and post-edge at 540 eV. The ratio of pre- and main-edge is important to evaluate O K-edge XAS of liquid water in transmission mode, and is proposed to be 0.38 [2]. Figure 2 shows the ratio of pre- and main-edge at different positions estimated by the O K-edge XAS shown in Fig. 1. The liquid thickness at different positions are also shown, which is estimated from the edge-jump and the absorption coefficient of liquid water. From 100 μm to 250 μm, the liquid thickness is nearly constant. The ratio of pre- and main-edge becomes 0.36-0.38 in this region. On the other hand, the liquid thickness is rapidly increased above 300 μm. The ratio of pre- and main-edge is also increased in this region. Because the beam size of soft X-rays is 200 × 200 μm^2, XAS in this region includes different thickness of liquid layers. The previous study suggests that the ratio of pre- and main-edge is increased at the mixtures of different thickness of the liquid layers [2].

In summary, we have developed the XAS measurement system that adjusts the liquid thickness by controlling not only the helium pressure to optimize the absorbance but also the sample position to find a flat area of the sample thickness.

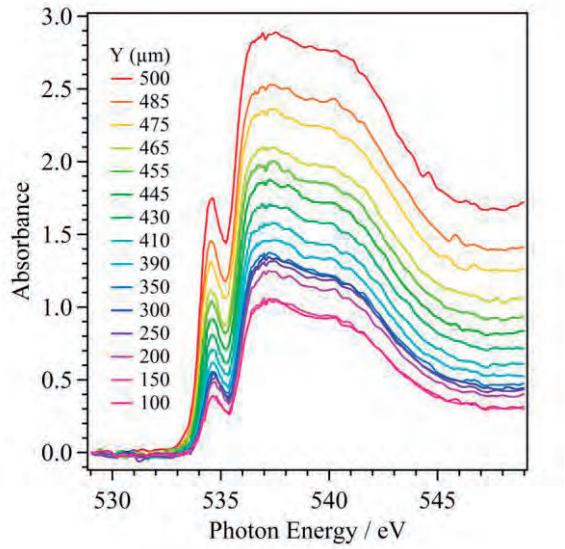

Fig. 1. O K-edge XAS spectra of liquid water at different sample positions (Y).

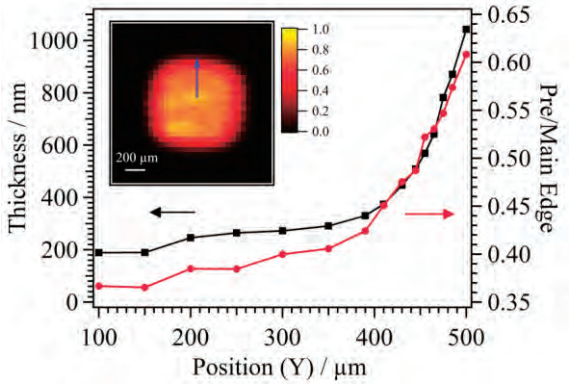

Fig. 2. Ratio of pre- and main-edge and the liquid thickness at different sample positions (Y) estimated from XAS shown in Fig. 1. The inset shows the images of X-ray transmission at 550 eV. The arrow indicates the sample position to measure XAS.

[1] M. Nagasaka *et al.*, J. Electron Spectrosc. Relat. Phenom. **177** (2010) 130.
[2] S. Schreck *et al.*, Rev. Sci. Instrum. **82** (2011) 103101.

BL3U

Detection of Intra- and Inter-Molecular Charge Transfer in Solution by N K-Edge X-Ray Absorption Spectroscopy

R. Golnak[1,2], J. Xiao[1], M. Tesch[1], M. Yablonskikh[1], M. Nagasaka[3], T. Brandenburg[1,4], N. Kosugi[3] and E. F. Aziz[1,2,3]

[1]*Institute of Methods for Material Development, Helmholtz-Zentrum Berlin für Materialien und Energie, Albert-Einstein-Straße 15, 12489 Berlin, Germany*

[2]*Department of Chemistry, Freie Universität Berlin, Takustraße 3, 14195 Berlin, Germany*

[3]*Institute for Molecular Science, Myodaiji, Okazaki 444-8585, Japan*

[4]*Department of Physics, Freie Universität Berlin, Arnimallee 14, 14195 Berlin, Germany*

Biological functions and chemical reactions mostly happen in solution. To understand these processes it is of paramount interest to know the electronic structure of liquids and solutions. Core level spectroscopy provides a probe to the electronic structure. In this work we investigated some derivatives of the Urea molecule (Fig. 1(A)) in water and in dimethyl sulfoxide (DMSO).

Through the measurements performed at the beamline BL3U at UVSOR-III we could obtain X-ray absorption (XA) spectra of the derivatives with sufficient signal intensity and without experimental saturation effects. These spectra are complemented by resonant inelastic X-ray scattering (RIXS) spectra obtained at the LiXEdrom endstation at BESSY II (Germany) [1, 2]. Partial fluorescence yield (PFY) measurements were also done at BESSY II to compare transmission mode absorption spectra obtained at UVSOR-III.

What we observed is that the different intra-molecular charge transfer, caused by different molecular dipole moments in these three species, leads to the energy shift of the N π* orbital below the ionization potential (IP) (Fig. 1(A)), while the different inter-molecular charge transfer, caused by different surrounding solvent dipoles, results in an energy shift of the N σ* orbital above the IP (Fig. 1 (B)). Occupied states are normally more localized in nature than the unoccupied states, and thus less influenced by the charge transfer effect, as shown in Fig. 2 that exhibits no energy shift between Urea and Thiourea for the occupied states. N K-edge XAS is sensitive to the molecular charge transfer, and therefore can be used as a good indicator detecting even minor changes of the chemical environment around the specific site of interest.

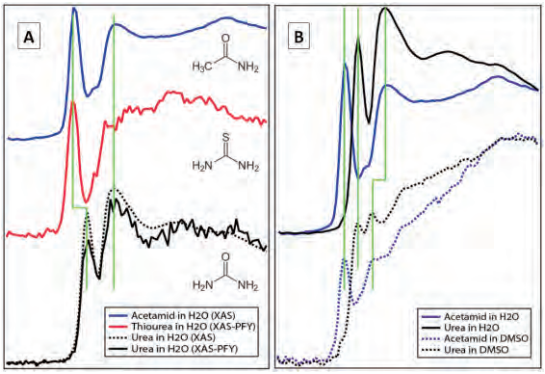

Fig. 1. (A) N π* orbital below IP, indicated by the left green line, has an energy shift, while N σ* above the IP, marked by the right green line, share the same energy. (B) Different solvents do not shift the N π* orbital, but the σ* instead, suggesting that the solvent only affects the orbital above the IP.

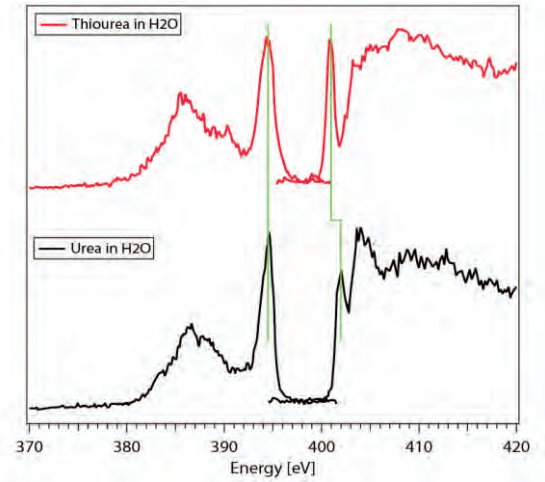

Fig. 2. Occupied states of Urea and Thiourea in water have almost identical energy positions, while the unoccupied states have an energy shift, as already discussed in Fig. 1 (A), resulting in an local energy gap opening for Urea, when compared with Thiourea.

[1] K. M. Lange *et al.*, Phys. Rev. B **85** (2012) 155104.

[2] C. Jung *et al.*, Nucl. Instrum. Methods Phys. Res. Sect. Accel. Spectrometers Detect. Assoc. Equip. **467-468** (2001) 485.

BL4U

Electrochemical Studies at BL4U STXM

S. M. Rosendahl[1,2], A. P. Hitchcock[1], M. Nagasaka[3], Y. F. Wang[3], T. Horigome[3], T. Ohigashi[3] and N. Kosugi[3]

[1] *Chemistry & Chemical Biology, McMaster University, Hamilton, L8S4M1, Canada*
[2] *Canadian Light Source, Saskatoon, SK S7N 5C9, Canada*
[3] *Institute for Molecular Science, Okazaki 444-8585, Japan*

UVSOR BL4U STXM provides chemical imaging with ~30 nm spatial resolution using 200-750 eV X-rays. This project uses STXM to investigate electrochemical systems, either prepared *ex situ* in defined electrochemical states, or with *in situ* modification of the electrochemical state of the system. Several generations of a device for *in situ* flow electrochemistry have been developed at UVSOR and in Canada. Here we report on progress in 2014, with data from two systems: (i) *in situ* solution oxidation of $FeSO_4$ (aq), and (ii) conversion of polyaniline (s) between emeraldine, the oxidized quinoid form and leucoemeraldine, the reduced aromatic form. Figure 1 is a photo of the latest version of the *in situ* UVSOR flow cell. Reproducible *in situ* flow in STXM has been achieved with this device but, for various reasons, an *in situ* data set has not yet been achieved.

In situ cyclic voltammetry and Fe 2p spectroscopy of $FeSO_4$ solutions have been carried out at BL3U using an electrochemical cell [1,2]. We have developed the Norcada/McMaster *in situ* cell from the concept of this cell [3]. This system was examined by STXM at the Fe 2p edge with *in situ* change of the electrochemical state. Figure 2a presents Fe $2p_{3/2}$ spectra of the reduced and oxidized Fe ions extracted from an image stack and set on an absolute intensity scale (OD per nm). The Fe $2p_{3/2}$ stack was fit to these spectra and a constant (water and Au electrodes), resulting in quantitative component maps which are presented as a color coded composite in Fig.2b. Surprisingly, the distribution of oxidation states was opposite that expected since the WE was positive relative to the CE when the stack was measured. It is also surprising that the solution has a redox gradient across it - one would expect diffusion to remove this. This, and the lack of blue tinge in the inter-electrode region, indicate there was very little water such that the solution phase is a gel.

Due to deterioration of the Au/Cr electrodes in Fe(II) solutions, the system used to further develop electrochemical STXM was changed to polyaniline (PANI), which has been studied with *in situ* STXM earlier [4]. However the 1 M HCl used as electrolyte damaged the stainless steel flow lines used in the UVSOR *in situ* flow cell (Fig. 1). We were only able to measure a dry sample, prepared *ex situ* at McMaster on an early 2-electrode chip ('PANI in a drop'). PANI was electrodeposited on the left electrode and left in the as-prepared oxidized state. PANI electrodeposited on the right electrode was electrochemically reduced after deposition. Figure 3a presents C 1s spectra of the oxidized and reduced states extracted from selected regions of the dry, *ex situ* sample, nice examples of the C 1s performance of the BL4U STXM. The spectra were used to fit C 1s stacks of the PANI deposits on each electrode; color coded composites are presented in Fig.3b &3b. The left electrode has only oxidized PANI, while the right electrode has a combination of reduced and oxidized PANI. The oxidized PANI is probably from PANI that was not electrically linked to the electrode.

Progress is steadily being made toward *in situ* flow electrochemical STXM at BL4U

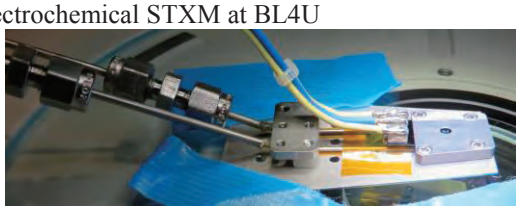

Fig. 1. photograph of the UVSOR *in situ* flow cell.

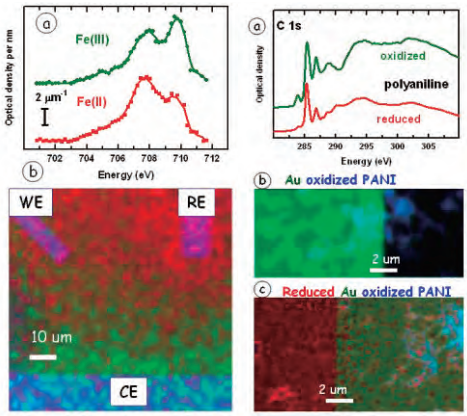

Fig. 2. **(a)** Fe(II) and Fe(III) spectra from stack of static cell with 0.1 M $FeSO_4$ (aq). **(b)** color coded composite of maps of Fe(II) (red), Fe(III) (green) and constant (blue) - electrodes.

Fig. 3. **(a)** C 1s spectra of *ex situ* deposited polyaniline, in the reduced and oxidized states. Color coded composites of **(b)** left, and **(c)** right electrodes which were converted electro- chemically to oxidized and reduced states in Canada.

[1] M. Nagasaka *et al.,* J. Phys. Chem. C **117** (2013) 16343.
[2] M. Nagasaka, Rev. Sci. Instrum. **85** (2014) 104105.
[3] A. P. Hitchcock *et al.,* J. Phys. Conf. Ser. (2015) in press.
[4] D. Guay *et al.,* Anal. Chem. **77** (2005) 3479.

BL4B

Stability of Molecular Dications Studied by an Electron-Electron-Ion Coincidence Method

K. Nakamura[1], R. Mashiko[1], K. Soejima[1], E. Shigemasa[2] and Y. Hikosaka[1]
[1]*Department of Environmental Science, Niigata University, Niigata 950-2181 Japan*
[2]*UVSOR Facility, Institute for Molecular Science, Okazaki 444-8585 Japan*

Inner-shell ionization of a molecule and subsequent Auger decay usually produce the doubly-charged molecular ion. The diaction is inherently unstable against the ion-pair dissociation, but it is known that, while the lifetime is of course state-dependent, some low-lying dication states can be metastable in micro second time scale or longer.

In this work, we have performed an electron-electron-ion coincidence study of the OCS diaction states. We have employed a magnetic-bottle electron spectrometer adapted to ion detection. The description is elsewhere [1]; here only brief accounts are given. The spectrometer equipped with a strong permanent magnet and a long solenoid coil, which create an inhomogeneous magnetic field forming a magnetic mirror to collect the electrons from almost the whole 4π solid angle. For coincidence detection of the counterpart ions, a pulsed high voltage was applied to the ionization region, according to an electron detection, and the formed ions were introduced into the same microchannel plate detector for electron detection.

Figure 1 shows a time-of-flight spectrum of electrons and ions produced from OCS at hν=318.6 eV. While electron structures are exhibited blew 4000 ns, the peaks due to molecular ions are observed later than 4000 ns. Figure 2 shows an energy correlation map displaying the correlations between S2p photoelectrons and Auger electrons. The horizontal axis covers an electron energy range in which the S2p photoelectrons appear, and the vertical axis does a range for the Auger electrons. At the photoelectron energies for the formations of the spin-orbit components of $S2p^{-1}$, several structures associated with different OCS^{2+} states are observed. The vertical cuts at the photoelectron energies are plotted with black and blue curves in Fig. 3, where two groups of peaks (0-4 eV and 4-10 eV) are observed. The red and green curves are the coincidence Auger spectra which are obtained by filtering with further coincidence with OCS^{2+} ions. In the coincidence spectra, the peaks in 4-10 eV are presented, but the peaks below 4 eV disappear. This observation implies that, while the states in the 4-10 eV range are metastable, the states in the 0-4 eV range have much shorter lifetimes.

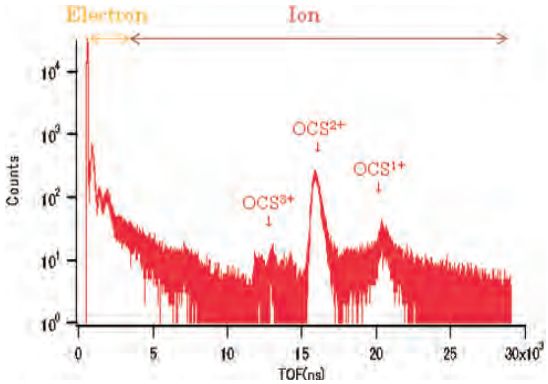

Fig. 1. Time-of-flight spectrum of electrons and ions produced from OCS at hν=318.6 eV.

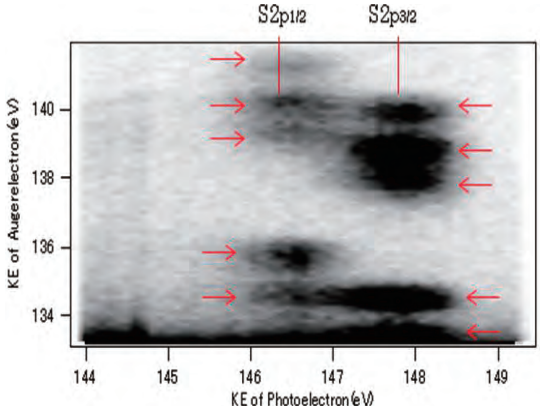

Fig. 2. Correlation map for ion pairs detected in coincidence with C1s photoelectron from CH_3OD.

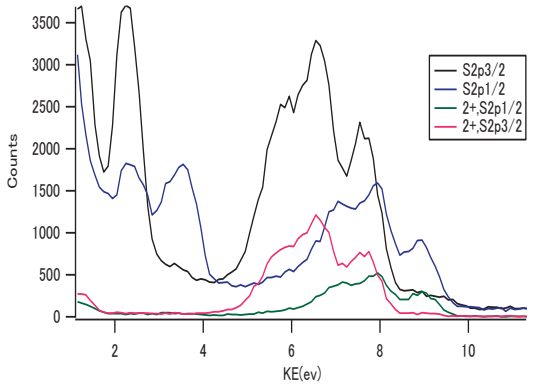

Fig. 3. Coincidence Auger spectra (black and blue) and those with further coincidence with OCS^{2+} ions (red and green).

[1] A. Matsuda, M. Fushitani, C.-M. Tseng, Y. Hikosaka, J. H. D. Eland and A. Hishikawa, Rev. Sci. Instrum. **82** (2011) 103105.

BL6U

Dissociation of CH_3OH Dication Studied by an Electron-Ion Coincidence Method

M. Higuchi[1], T. Shirota[2], K. Hoshina[2], H. Iwayama[3], E. Shigemasa[3] and Y. Hikosaka[1]

[1]*Department of Environmental Science, Niigata University, Niigata 950-2181, Japan*

[2]*Faculty of Pharmaceutical Sciences, Niigata University of Pharmacy and Applied Life Sciences, Niigata 956-8603, Japan*

[3]*UVSOR Facility, Institute for Molecular Science, Okazaki 444-8585, Japan*

Molecular absorption of a soft x-ray photon often induces inner-shell photoionization, and the formed core-hole usually relaxes via Auger decay. Because two electrons are emitted through this sequential process, the molecule with two positive charges is produced. This dication is inherently instable due to the Coulomb repulsion of the two positive charges, and thus most of the dication states dissociate into ion pairs. In this work, we have studied the ion-pair dissociation of the CH_3OH dication states, by an electron-ion coincidence method.

The experiment was performed at the undulator beamline BL6U. We utilized an electron-ion coincidence spectrometer [1,2] composed of a toroidal electron analyzer and ion momentum imaging analyzer. Figure 1 shows time-of-flight spectra of ions produced after the C1s inner-shell ionization of CH_3OH and CH_3OD, observed in coincidence with C1s photoelectrons emitted at hν= 292.3 eV. While the structure around 2340 ns in the CH_3OH spectrum is allocated to the OH^+ fragments, the CH_3OD spectrum also shows sizable intensity in the same TOF range. In addition, the structure due to the OD^+ fragments can be observed around 2410 ns in the CH_3OD spectrum. These observations imply that the hydrogen atom in the OH^+ fragment is not always the one originally placed at the oxygen side in the neutral ground state of CH_3OH, and thus suggests that the molecular structure can be largely deformed in the dissociation pathway producing the OH^+ fragment.

The correlation map in Fig. 2 presents ion pairs detected in coincidence with C1s photoelectron from CH_3OD. One finds on the map structures corresponding to the ion pairs of $OD^+ + CH_2^+$ and $OH^+ + CDH^+$. While the former ion pair can be produced by a simple CO bond breaking, the formation of latter needs a hydrogen exchange before the bond breaking.

Figure 3 shows coincidence Auger spectra (red) which are filtered by detections with $OD^+ + CH_2^+$ and $OH^+ + CDH^+$, compared to the normal Auger spectrum (black). The coincidence Auger spectrum associated with $OD^+ + CH_2^+$ (simple CO bond breaking case) shows a peak at 41.3 eV. On the other hand, the peak location is 39.3 eV in the coincidence Auger spectrum associated with $OH^+ + CDH^+$ (hydrogen exchange case). This observation implies that fairly-stable dication state(s) lies around 39.3 eV, where hydrogen exchange precedes the bond breaking.

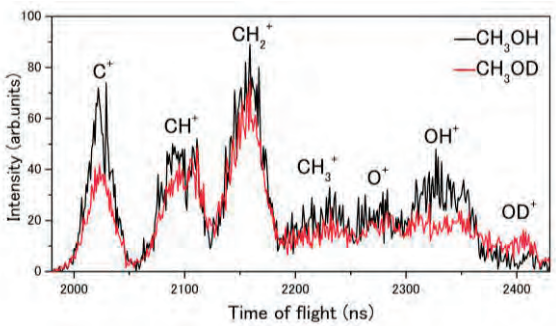

Fig. 1. Time-of-flight spectra of ions produced after the C1s inner-shell ionizations of CH_3OH (black) and CH_3OD (red), observed in coincidence with C1s photoelectrons emitted at hν=292.3 eV.

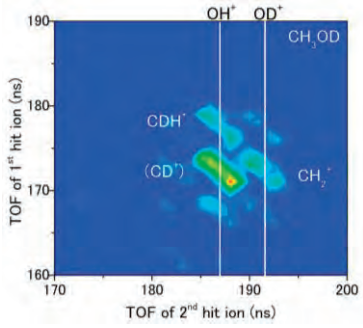

Fig. 2. Correlation map for ion pairs detected in coincidence with C1s photoelectron from CH_3OD.

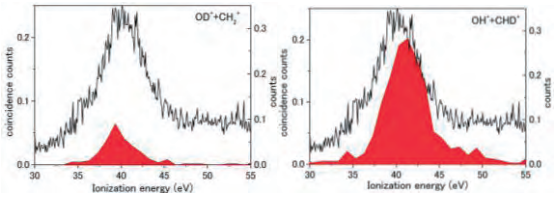

Fig. 3. Coincidence Auger spectra (red) which are filtered by detections with $OD^+ + CH_2^+$ and $OH^+ + CDH^+$, compared to the normal Auger spectrum (black).

[1] T. Kaneyasu, Y. Hikosaka and E. Shigemasa, J. Electron Spectrosc. Rel. Phenom. **156-158** (2007) 279.

[2] Y. Hikosaka, Y. Shibata, K. Soejima, H. Iwayama and E. Shigemasa, Chem. Phys. Lett. **603** (2014) 46.

BL6U

Spectator Auger Decays of 1,1,1-Trifluoroethane across the F K Threshold

T. Kaneda[1], K. Okada[1], H. Iwayama[2,3] and E. Shigemasa[2,3]

[1]*Department of Chemistry, Hiroshima University, Higashi-Hiroshima 739-8526, Japan*

[2]*UVSOR Facility, Institute for Molecular Science, Okazaki 444-8585, Japan*

[3]*School of Physical Sciences, The Graduate University for Advanced Studies (SOKENDAI), Okazaki 444-8585, Japan*

Inner-shell excitation of gaseous molecules results in a specific dissociation through Auger processes. Recently, we found in the F KVV Auger spectra of *cis*-hexafluorocyclobutane (*cis*-c-$C_4H_2F_6$, HFCB) that spectator decay predominates and that the peaks change almost linearly with photon energy [1]. These shifts are known as "spectator shifts" arising from the core-hole screening of a spectator electron for an outgoing electron. In addition to the spectator shifts, a fluorine atomic Auger peak was observed. This peak implies the presence of ultrafast dissociation (UFD). It takes place during the lifetime of the core-hole state before Auger electron emission. It is rare that the UFD can be observed clearly in relatively large molecules.

In this study, to investigate spectator shifts quantitatively, we measured resonant/normal Auger spectra of 1,1,1-trifluoroethane (CH_3CF_3) across the F K threshold as a function of photon energy with a small energy step and a higher electron energy resolution. Because the CH_3CF_3 molecule has a higher symmetry than that of HFCB, we expect a simple spectrum, making spectator shifts clearer.

The experiments were performed on the soft X-ray beamline BL6U. A main chamber was equipped with a high-resolution hemispherical electron analyzer (MBS-A1). The monochromatized radiation was focused onto a center of a gas cell containing the sample gas and the pressure of the main chamber was kept at 1.0×10^{-3} Pa during the measurements. Electron spectra were recorded in the F 1s region ($h\nu$ = 682.0–702.0 eV) with a photon energy step of 0.5 eV.

Figure 1 shows some of the resonant/normal Auger spectra plotted on the electron kinetic energy scale. The spectra have been obtained by subtracting the contribution from the photoelectron acquired at $h\nu$ = 683.0 eV. The spectator shifts can be evaluated using the F 1s ionization threshold of CH_3CF_3: 694.1 eV [2]. One can see that the electronic relaxation processes are dominated by spectator Auger decay, in contrast with low probability of participator Auger decay. This is the same trend as in the case of HFCB [1]. On the analogy of HF [3], we assign the intense bands around 650, 625 and 605 eV to the transitions to the final state of $v_o^{-1}v_o^{-1}$, $v_o^{-1}v_i^{-1}$ and $v_i^{-1}v_i^{-1}$, respectively. The notation v_o represents an outervalence orbital such as F 2p, and v_i is an innervalence. The positions of spectator Auger bands (S1–S3) shift with the photon energy leading to the normal Auger bands (N1–N3). This is similar to the results of HFCB, but the positions seem to vary in a non-linear manner because each of these spectator peaks is composed of several components. In addition, the shapes of these spectra change dramatically with the excitation energy. We need to find the correct components to evaluate the spectator shifts. The analysis is in progress now.

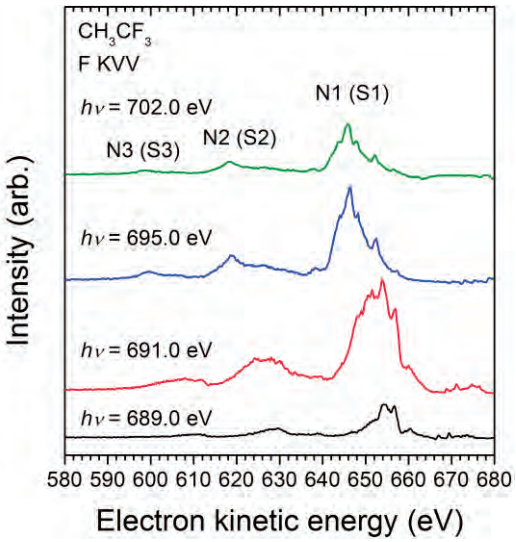

Fig. 1. Resonant and normal Auger spectra of CH_3CF_3 acquired at some photon energies across the F K threshold.

[1] T. Kaneda, S. Ishikawa, K. Okada, H. Iwayama, L. Ishikawa and E. Shigemasa, UVSOR Activity Report 2013 **41** (2014) 119.

[2] W. L. Jolly, K. D. Bomben and C. J. Eyermann, At. Data Nucl. Data Tables **31** (1984) 433.

[3] R. W. Shaw, Jr. and T. D. Thomas, Phys. Rev. A. **11** (1975) 1491.

BL6U

Specific Auger Decay and Photofragmentation of *cis*-Hexafluorocyclobutane

S. Ishikawa[1], K. Okada[1], H. Iwayama[2,3] and E. Shigemasa[2,3]

[1]*Department of Chemistry, Hiroshima University, Higashi-Hiroshima 739-8526, Japan*

[2]*UVSOR Facility, Institute for Molecular Science, Okazaki 444-8585, Japan*

[3]*School of Physical Sciences, Graduate University for Advanced Studies (SOKENDAI), Okazaki 444-8585, Japan*

Inner-shell excited states of molecules relax into various molecular cationic states through Auger decays. The resultant cations are in general unstable and dissociate into fragment ions. In our previous study we observed site-specific fragmentation of the inner-shell excited *cis*-hexafluorocyclobutane (HFCB, *cis*-c-$C_4H_2F_6$) molecule. The yield spectra of the fragment ions with C–F bond(s) have a peak at the σ_{CC}^* resonance, while those of the ions without C–F bonds do not. This infers that the resonant state decays to particular Auger-final states, connecting to specific fragmentation channels. The purpose of this study is to illuminate such Auger processes with the measurements of Auger-electron–photoion coincidence (AEPICO) spectra.

The experiments have been performed on the soft X-ray beamline BL6U. The experimental setup has been described in a previous report [1]. Synchrotron radiation was irradiated at right angles to the effusive beam of the gaseous HFCB sample. The electrons traveling through a double toroidal analyzer tube were detected with a position sensitive detector (RoentDek, DLD40). The pass energy was set to 400 eV in this study. Photofragment ions were extracted toward the time-of-flight spectrometer by a pulsed electric field applied just after the Auger electron detection. The light intensity was monitored downstream on the beamline during the measurements. The coincidence data were acquired at the photon energies of 707.5, 695.0, 688.5, 310.0, 297.0 and 292.8 eV.

The branching fraction of the Auger processes is found to depend on the resonant states. Figure 1a shows some typical resonant Auger spectra plotted on the final-state energy scale. The normal Auger spectrum measured under the same experimental conditions is also given at the top on the double ionization energy scale. Two peaks are found in this energy range. They are assigned to spectator Auger decays [2]. The intensity ratio of the two peaks varies with the photon energy: 0.36 at 707.5 eV, 0.33 at 695.0 eV and 0.41 at 688.5 eV. This indicates that the presence of a spectator electron clearly affects the Auger decays.

A noticeable feature can be seen in the coincidence spectra. Panel b shows the Auger electron yield curves coincident with the $C_2H_{0,1}F^+$ and $C_2H_{0\text{-}2}^+$ ions, which have been obtained by editing the AEPICO data acquired at 695.0 eV. Auger electrons forming the S2 peak are almost exclusively coincident with the ions without C–F bonds, except for $CH_{0,1}F^+$ (not shown in Fig. 1). This fact represents that the suppression of the S2 peak is responsible for the site-specific fragmentation at the F K-edge: smaller branching fraction to form the S2 peak makes the yield of the ions without C–F bonds lower.

The resonant Auger spectra at the C K-edge are in clear contrast to those at the F edge. The spectrum for the σ_{CC}^* resonance at 297.0 eV has a strong, broad peak at around the final-state energy of 40 eV. Abundant photofragments in coincidence with the corresponding Auger electrons are the ions with C–F bond(s). The processes to show the site specificity are different between at the F edge and at the C edge.

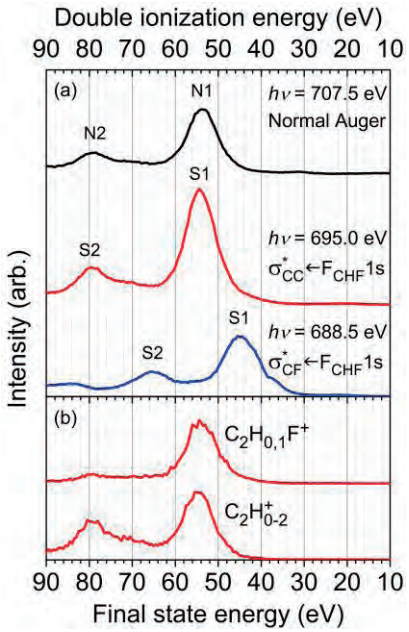

Fig. 1. Resonant and normal Auger spectra of HFCB measured at three excitation energies (a) and the components coincident with $C_2H_{0,1}F^+$ and $C_2H_{0\text{-}2}^+$ at the photon energy of 695.0eV (b).

[1] S. Ishikawa, K. Okada, H. Iwayama, L. Ishikawa and E. Shigemasa, UVSOR Activity Report 2012 **40** (2013) 58.

[2] T. Kaneda, S. Ishikawa, K. Okada, H. Iwayama and E. Shigemasa, UVSOR Activity Report 2013 **41** (2014) 119.

BL6U

Ultrafast Dissociation of Core Excited CF_4 Molecules Studied by an Auger-Electron–Ion Coincidence Method

H. Iwayama[1,2] and E. Shigemasa[1,2]

[1]*UVSOR Facility, Institute for Molecular Science, Okazaki 444-8585, Japan*

[2]*School of Physical Sciences, The Graduate University for Advanced Studies (SOKENDAI), Okazaki 444-8585, Japan*

Molecular inner-shell excitation into an anti-bonding orbital causes a nuclear motion. In some cases, the nuclear dynamics is so fast that dissociation takes place before Auger electron emission. This process is referred to as ultrafast dissociation and observed in hydrogen halide molecules such as HBr [1] and HCl [2].

Recently, we found a signature of ultrafast dissociation following C 1s→$\sigma^*(t_2)$ core excitation in CF_4 by using two dimensional electron spectroscopy [3]. We observed Auger electrons from both CF_3* fragment and CF_4* parent molecule. This means that the Auger decay and dissociation processes take place on the same time scale and significantly compete with each other.

In the present work, we have investigated anisotropic angular distributions of ejected CF_3^+ ions by using an Auger-electron–ion coincidence method. Since the CF bond involved in the C 1s→σ*(t2) core excitation is immediately broken due to the ultrafast dissociation, anisotropic angular distributions of ejected the CF_3^+ ions are expected.

The Auger-electron–ion coincidence measurements were carried out on the undulator beamline BL6U at UVSOR. The radiation from an undulator was monochromatized by a variable included angle varied line-spacing plane grating monochromator. The electrons ejected at 54.7° with respect to the electric vector of the incident radiation were analyzed in energy by a double toroidal analyzer (DTA), while ions were extracted from the interaction region into a momentum spectrometer by a pulsed electric field according to the electron detection. Arrival position on the detector and time-of-flights of ions were recorded for every event. The pass energy of the DTA was set to 200 eV for observing the Auger electrons. The energy resolution was about 1.9 eV. All signals from the detectors were recorded with an 8ch TDC board. We used the photon energy of 298.5 eV, which corresponds to the C 1s → $\sigma^*(t_2)$ resonance.

Figure 1 shows total and coincidence Auger spectra with CF_3^+ ions. It is seen that the CF_3^+ ions are coincident with electrons at the binding energy of 15~25 eV, where two peaks A and B are detected. For higher binding energies, we observed smaller fragment ions such as CF_2^+, CF^+ and C^+ (not shown here). From the previous work [3], the peaks A and B are attributable to the Auger electrons from the CF_3^* fragment and CF_4^* parent molecules, respectively.

Figures 2(a) and 2(b) show ion images of CF_3^+ ion fragments, which were taken in coincident with electrons at the peaks A and B, respectively. The angular distribution of CF_3^+ ions is considerably anisotropic in Fig. 2(a), while almost isotropic angular distributions are seen in Fig. 2(b). Two island-like structures along the polarization vector are clearly observed in Fig. 2(a). This means that the core-excited CF_4 molecules lead to immediate CF bond breaking, which is the direct evidence of the ultrafast dissociation for the peak A. The detailed data analyses are now in progress.

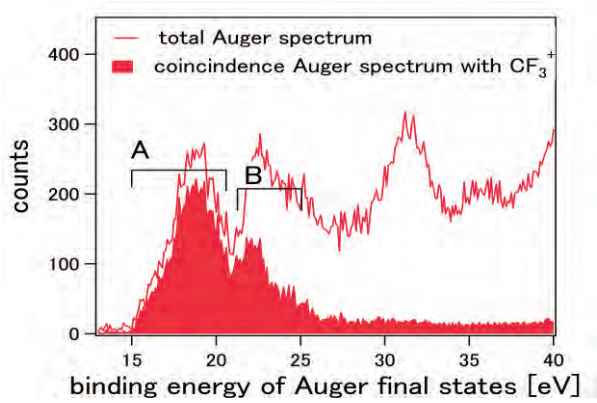

Fig. 1. Total and coincident Auger electron spectrum with CF_3^+ ions.

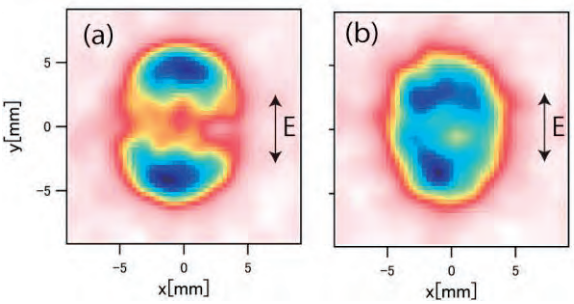

Fig. 2. Ion images of CF3+ ions coincident with Auger electrons at (a) peak A and (b) peak B.

[1] M. Morin and I. Nenner Phys. Rev. Leet. **56** (1986) 1913.
[2] H. Aksela *et al*., Phys. Rev. A **41** (1990) 600.
[3] M. N. Piancastelli, R. Guillemin, M. Simon, H. Iwayama and E. Shigemasa, J. Chem. Phys. **138** (2013) 23430.